Hydrolysis of Phosphatidylcholine by Hepatic Lipase in Discoidal and Spheroidal Recombinant High-Density Lipoprotein†

John T. Tansey,*,‡ Tom Y. Thuren,‡,§,|| W. Gray Jerome,§,⊥ Roy R. Hantgan,‡,§ Ken Grant,⊥ and Moseley Waite‡,§

Departments of Biochemistry, Medicine, and Pathology, Bowman Gray School of Medicine, Winston-Salem, North Carolina 27157-1016

Received February 17, 1997; Revised Manuscript Received July 25, 1997⊗

ABSTRACT: Hepatic lipase (HL) hydrolysis of phosphatidylcholine (PC) was studied in recombinant high-density lipoprotein particles (r-HDL). r-HDL were made from cholate mixed micelles that contained PC, apo AI, and, in some cases, unesterified cholesterol. r-HDL were characterized using chemical composition, nondenaturing gradient gel electrophoresis, transmission electron microscopy, and dynamic light scattering. The r-HDL were found to be discoidal and in the size range of native HDL. Upon treatment of cholesterol-containing r-HDL with lecithin−cholesterol acyltransferase (LCAT), to form cholesteryl ester, the discoidal r-HDL became spheroidal. The effects of r-HDL morphology and size on HL activity were studied on r-HDL made of palmitoyloleoyl-PC, unesterified cholesterol, cholesteryl ester, and apolipoprotein AI. Spheroidal r-HDL were hydrolyzed at a faster rate than discoidal r-HDL. Protein-poor r-HDL were hydrolyzed by HL at a faster rate than protein rich r-HDL. Unesterified cholesterol had no apparent effect on particle PC hydrolysis. The hydrolysis of different species of PC [dipalmitoyl (DPPC), dioleoyl- (DOPC), palmitoylarachidonoyl (PAPC), and palmitoyloleoyl (POPC)] in r-HDL was also investigated. In discoidal r-HDL, we found that POPC ≥ DOPC = PAPC/DPPC. However, in LCAT-treated spheroidal r-HDL, POPC = DOPC > PAPC/DPPC. In both discoidal and spheroidal rHDL, DPPC containing r-HDL were not hydrolyzed to a significant extent. Collectively, these studies demonstrate that the physico−chemical properties of particles (such as phospholipid packing and phospholipid acyl composition) play a significant role in hydrolysis of HDL phospholipid by HL and, therefore, in reverse cholesterol transport.

Hepatic lipase (HL)[1] (Waite & Sisson, 1973) is a multifunctional lipase found on the surface of the liver sinusoid (Kuusi *et al.*, 1979). One of HL's functions is the catabolism of the PL coat of HDL. This results in the uptake of HDL CE by the hepatocyte (Bamberger *et al.*, 1983,1985; Marques-Vidal *et al.*, 1994; Kadowaki *et al.*, 1992). Individuals exhibiting HL deficiency experience an above-normal risk of premature atherosclerosis as well as elevated HDL levels (Hegele *et al.*, 1993; Connelly *et al.*, 1990; Goldberg *et al.*, 1985; Breckenridge *et al.*, 1982). Similarly, mice in which the HL gene has been deleted have increased HDL cholesterol levels whereas mice and rabbits that express human HL have decreased levels of HDL cholesterol (Busch *et al.*, 1994; Homanics *et al.*, 1995; Fan *et al.*, 1994).

A paradox exists in that while the liver is a site of HDL catabolism it is also the site of HDL production. Disk-shaped HDL are found in monkey liver perfusates suggesting they are the nascent form of HDL (Babiak *et al*., 1986; Johnson *et al.*, 1986). These particles are also found in familial LCAT deficiency (Forte *et al.*, 1971). LCAT acts on discoidal particles by esterifying the hydroxyl moiety of UC with an acyl chain derived from the *sn*-2 position of PC, thereby forming lyso-PC and CE. It is known that discoidal HDL are an excellent substrate for LCAT (McCall *et al.*, 1993; Babiak *et al.*, 1986).

Discoidal HDL are modeled as a bilayer of PL and UC surrounded by the amphipathic α helices of apo AI which shield the hydrophobic acyl chains of PL from the aqueous surroundings (Hamilton *et al.*, 1976). We hypothesize that the packing of the lipid in disks inhibits the hydrolysis of PL by HL, ensuring that newly formed particles can escape from the liver sinusoids to the circulation. LCAT action on disks results in production of CE which begins to form a hydrophobic core in the particle (Albers *et al.*, 1986), a process we believe will decrease the lateral surface pressure of the PL molecules. This is not only due to the loss of PC and UC as the result of LCAT action but also due to a gradual change from a bilayer to a curved monolayer of PL surrounding a CE-rich core (Verdery & Nichols, 1975). Based on studies that employed monolayers of PL, we know that HL can more readily penetrate and hydrolyze PL surfaces with lower lateral surface pressure. HL has optimal activity at surface pressures of 15−25 mN/m and is no longer active at 30 mN/m (Thuren *et al.*, 1992).

In this work, we compared the hydrolysis rates of PC in various well characterized types of r-HDL. PC has been

† We acknowledge the support of the Analytical Chemistry and Electron Microscopy Core Laboratories of the Comprehensive Cancer Center. This work was supported by Grant HL48077 from the NIH.

* To whom correspondence should be addressed. Telephone: (910) 716-4329. Fax: (910) 716-7671.

‡ Department of Biochemistry.

§ Members of the Comprehensive Cancer Center of Wake Forest University.

|| Department of Medicine.

⊥ Department of Pathology.

⊗ Abstract published in *Advance ACS Abstracts,* September 15, 1997.

[1] Abbreviations: HL, hepatic lipase; POPC, palmitoyloleoylphosphatidylcholine; PAPC, palmitoylarachidonoylphosphatidylcholine; DOPC, dioleoylphosphatidylcholine; DPPC, dipalmitoylphosphatidylcholine; UC, unesterified cholesterol; CE, cholesteryl ester; PC, phosphatidylcholine; PE, phosphatidylethanolamine; PL, phospholipid; apo AI, apolipoprotein AI; LCAT, lecithin−cholesterol acyltransferase; r-HDL, recombinant high-density lipoprotein; GGE, gradient gel electrophoresis; EM, electron microscopy; DLS, dynamic light scatter; SDS−PAGE, sodium dodecyl sulfate−polyacrylamide gel electrophoresis.

S0006-2960(97)00356-5 CCC: $14.00

chosen as the type of PL used to form r-HDL based on its relative abundance (80% of PL) in the PL coat of native HDL as well as its particle-forming properties. The PC:FC:AI ratios were chosen based on values cited in the literature which facilitated r-HDL formation. Final ratios of components were slightly enriched in PC and depleted in FC and CE compared to native HDL but were still in the range of native HDL and provided a viable model for the native particle. By using particles of a defined nature, many of the complications arising from conformational, compositional, and size heterogeneity can be avoided. We report that spheriodal, large, CE-rich particles are the preferred substrate for HL.

MATERIALS AND METHODS

Materials

Preparations of POPC, DPPC, and PAPC were obtained from Avanti Polar Lipids (Birmingham, AL). Cholesterol was obtained from Sigma (St. Louis, MO). Methyl iodide, ^{3}H-labeled (50−100 mCi/mmol); [*dipalmitoyl*-1-^{14}C]DPPC (80−120 Ci/mmol); and [*arachidonoyl*-1-^{14}C]PAPC, (50−60 Ci/mmol) were purchased from American Radiolabeled Chemicals (St. Louis, MO) whereas radiolabeled [*dioleoyl*-1-^{14}C] DOPC (80−120 Ci/mmol); cholesterol, [4-^{14}C] (45−60 Ci/mmol); and cholesterol, [7-^{3}H(N)](10−30 Ci/mmol) were obtained from DuPont, New England Nuclear (Boston, MA). Heparin−agarose, Sephacryl S-200, DEAE-Sephacel, and Phast Gel electrophoresis media were obtained from Pharmacia Biotech (Uppsala, Sweden). Biobeads were purchased from Bio Rad (Hercules, CA). Silica gel G thin-layer chromatography plates were purchased from Analtech (Newark, DE). All other supplies and reagents were purchased from either Sigma or Fisher.

Methods

Synthesis of Radiolabeled POPC. POPC was synthesized by methylation of POPE using [^{3}H]methyl iodide by the method of Patel *et al.* (1979).

Purification of Apo AI. Apo AI was isolated by the method of Brewer *et al.* (1986) from recovered plasma obtained from the American Red Cross. HDL were isolated by flotation ultracentrifugation in a KBr gradient and subsequently delipidated using a 2:1 ratio of $CHCl_3$/CH_3-OH. Apo AI was then purified using size exclusion chromatography (Sephacryl S-200, run in a buffer of 50 mM glycine, 4 mM NaOH, 0.5 M NaCl, and 6 M urea, pH 8.8). The isolated apo AI in 100 mL was dialyzed against 4 changes of 4 L of 10 mM NH_4HCO_3 and lyophilized. The lyophilized powder was resuspended in 10 mM NH_4HCO_3 prior to use. The purity of apo AI was assayed using SDS−PAGE stained with silver and found to be greater than 95%.

HL Purification. HL was purified by our modification (Waite *et al.*, 1991) of the procedures of Jensen and Bensadoun (1981) and Ehnholm and Kuusi (1986). In our procedure, rat liver is perfused with a heparin-containing Krebs−Ringer buffer to dissociate HL from the surface of the liver. HL is purified using heparin affinity chromatography followed by DEAE-Sephacel affinity chromatography. HL appeared as a single band on SDS−PAGE following purification.

Preparation of r-HDL. r-HDL particles were prepared by the procedure of Sparks *et al.* (1992) with the following modifications: UC was included in some preparations as noted. The PC:cholate ratio used was varied between 0.74:1 and 0.5:1 to optimize solution-clearing and r-HDL formation, and the amount of biobeads used was decreased to 50 mg of biobeads/mg of cholate. Following cholate removal, r-HDL were separated from biobeads using a 0.22 μm filter (Gelman Sciences). As determined by using radiolabeled cholate, greater than 99.5% of cholate was removed by the biobeads (data not shown). r-HDL were isolated by KBr density gradient ultracentrifugation prior to further use. In this centrifugation, the density of the r-HDL was adjusted to 1.22 g/mL using solid KBr. The gradient consisted of 5 mL of $d = 1.22$ g/mL, 5 mL of $d = 1.063$ g/mL, and 2 mL of $d = 1.019$ g/mL. The gradient was centrifuged at 35 000 rpm for 16 h in a SW-41 rotor. Fractions were collected manually from the top (lowest density) to the bottom (greatest density) of the gradient.

Transformation of r-HDL. Half of each preparation of r-HDL was converted from disks to spheres using LCAT which transfers the acyl chain from the *sn*-2 position of PC to the free hydroxyl group of UC forming CE (Nichols *et al.*, 1985). Medium from a stably transfected CHO cell line overexpresing LCAT (generously provided by Dr. Mary Sorci-Thomas, Bowman Gray School of Medicine) was incubated with particles for 6 h at 37 °C in 14 mM β-mercaptoethanol. Following the reaction, the same gradient ultracentrifugation as above was performed to reisolate particles.

Particle Characterization. Recombinant complexes were characterized using the following methods. PL and total cholesterol were determined using the specific radioactivity of the lipid. The CE content was determined by separating CE from UC by TLC [hexanes/isopropyl ether/acetic acid (60:40:3)]. Protein was determined using Petersen's (1977) modification of the Lowry *et al.* (1951) protocol. Native GGE was performed using a Pharmacia Phast Gel electrophoresis system with 8−25% polyacrylamide gels. Proteins were visualized by silver staining (Pharmacia Phast Gel Silver Stain Kit). EM was performed on particles negatively stained with 2% phosphotungstic acid and viewed with a Phillips TEM-400 at 55 000 × magnification. Particles were isolated on formvar-coated copper grids prior to staining. For the purpose of quantitation, the length and width of 50 particles were measured.

Dynamic Laser Light Scattering. The distribution of particle sizes was measured by dynamic light scattering performed with a Brookhaven Instruments BI2030AT correlator, operated in conjunction with a BI-200 SM light scattering goniometer/photon counting detector and a Spectra Physics 127 He−Ne laser (35 mW, equipped with a vertical polarization rotator) (Hantgan *et al.*, 1993). Data were collected at a 90° scattering angle, and particle size distributions were extracted from the resulting autocorrelation functions using the CONTIN algorithm (Provencher, 1982).

Particle Hydrolysis by HL. Two hundred nanomoles of PC in r-HDL particles was hydrolyzed by 0.6 μg of HL in 100 mM Tris, pH 9.0, containing 125 mM of NaCl, 12.5 mg fatty acid free bovine serum albumin, 0.3% glycerol, 100 units of heparin, 0.002% EDTA, and 0.01% NaN_3 for 1 h. After the incubation, the reaction was stopped by the addition of 3 mL of chloroform/methanol (1:2 v/v). Products of the reaction were separated by TLC [chloroform/methanol/ammonium hydroxide/water (60:40:3:2, v/v)], and the ra-

Table 1: Composition of POPC Particles with Differing Size and Free Cholesterol Content

starting ratio, PC:FC:AI	LCAT	mol % CE	final ratio PC	FC	CE	AI
100:0:1	+	0	101 ± 32	0	0	1
	−	0	111 ± 23	0	0	1
100:10:1	+	9	114 ± 6	0	11 ± 1	1
	−	0	117 ± 12	10 ± 2	0	1
100:20:1	+	15 ± 4	122 ± 16	5 ± 4	22 ± 8	1
	−	0	130 ± 29	27 ± 9	0	1
28:5.6:1	+	12	55 ± 5	3 ± 1	8 ± 1	1
	−	0	55 ± 2	12 ± 2	0	1

[a] The compositions of r-HDL made with POPC were determined. Starting ratio indicates the starting ratio of particle components to one another. LCAT indicates whether the r-HDL were treated with LCAT (+) or left untreated (−); mol % CE indicates the mole percent CE in each type of particle. Final ratio of PC:FC:CE:AI lists the ratio of components in the isolated r-HDL normalized to one molecule of apo AI. r-HDL components were determined using techniques described under Methods. Values are expressed as mean ± SEM of separate experiments (inter-experimental error).

diolabeled products (PC and lyso-PC) were scraped from the plate and quantitated using liquid scintillation counting. Hydrolysis of a mixed micelle of monoolein and Triton X-100 (1 μmol of monoolein in a 10:1 ratio with Triton) was used as a positive control (Waite *et al.*, 1991).

RESULTS

Molecular complexes of PC, UC, and apo AI r-HDL were isolated by density gradient ultracentrifugation (data not shown). This procedure ensured the separation of both unassociated lipid and protein from the r-HDL that was recovered from fractions 5−9. Unassociated lipid was found at the top of the gradient as determined by radioactivity; unassociated protein was found at the bottom of the gradient using Petersen's (1977) protein assay. UC was enriched in the less dense (front) half of the peak. As expected, r-HDL which were lipid-poor (28:5.6:1 starting ratio) floated at a higher density than lipid-rich r-HDL (100:20:1 starting ratio). Fractions 5−9 were pooled in all cases to cover the density range of all particles made for this study. Ultracentrifugations were also performed in a similar fashion after treatment with LCAT to reisolate the r-HDL. In these cases, the peak was somewhat broader in LCAT-treated samples than the untreated disks, which remained unchanged. Control incubations showed that following reisolation there was no LCAT activity associated with r-HDL. Lyso-PC formed in the LCAT reaction was distributed evenly throughout the gradient and not associated specifically with particles as determined by quantitation of lyso-PC from radioactivity following TLC of gradient fractions.

The chemical composition of r-HDL is given in Tables 1−3 for r-HDL made with varying ratios of PC to UC to apo AI and different species of PC. The data show that the final ratios of components did not change significantly from the starting ratios. Treatment of disks with LCAT resulted in esterification of 80% or greater of the UC in POPC r-HDL, and greater than 15 mol % of the lipid in 100:20:1 POPC r-HDL was CE. When the lipid to apo AI ratio was decreased to 28:5.6:1, the resulting r-HDL had the expected low lipid content although on LCAT treatment they had a mole percent CE that approached the amount found in the r-HDL with a ratio of 100:20:1 (15 ± 4 *vs* 12). When other molecular species of PC were used, less UC was incorporated and esterified in the r-HDL when compared to POPC (Table 3).

Table 2: Hydrolysis of Disks with Differing Acyl Composition

acyl composition	final ratio, PC:AI	nmol of PC hyd min^{-1} (mg of HL)$^{-1}$
POPC	(111 ± 23):1	330 ± 60
DOPC	(128 ± 20):1	280 ± 40
PAPC	(106 ± 2.1):1	190 ± 80
DPPC	111:1	0.0

[a] r-HDL disks made without FC were hydrolyzed by HL using the conditions cited under Methods. Final ratio of PC:AI lists the final ratio of components to one another normalized to one molecule of apo AI. Nanonmoles of PC hydyolyzed per minute per milligram of HL lists the rate of PC hydrolysis. Three experiments were performed in duplicate. Values given are expressed as mean ± SEM.

Table 3: Composition and Hydrolysis of Particles with Cholesterol and Differing Acyl Content

acyl composition	LCAT	mol% CE	starting ratio PC	FC	CE	AI	nmoles PC hyd./min/ mg HL
POPC	+	14.2	86	1	14	1	260 ± 20
	-	0	89	12	0	1	110 ± 0
DOPC	+	9 ± 4	63 ± 2	1 ± 2	6 ± 2	1	190 ± 90
	-	0	77 ± 4	9	0	1	70 ± 30
PAPC	+	9 ± 3	60 ± 7	1 ± 2	6 ± 2	1	120 ± 10
	-	0	79 ± 13	8 ± 1	0	1	90 ± 10
DPPC	+	4	94 ± 14	6 ± 2	4	1	0.0
	-	0	86 ± 2	8 ± 1	0	1	0.0

[a] r-HDL were characterized and hydrolyzed using the conditions listed under Methods. LCAT indicates whether the r-HDL were treated with LCAT (+) or left untreated (−). mol % CE indicates the mole percent CE in each type of particle. Final ratio of PC:FC:CE:AI lists the final ratio of components to one another normalized to one molecule of apo AI. r-HDL components were determined using techniques described under Methods. Nanomoles of PC hydrolyzed per minute per milligram of HL lists the rate of substrate hydrolysis Three experiments were performed in duplicate. Values are expressed as mean ± SEM.

Nondenaturing GGE was also used to characterize all r-HDL. In r-HDL made with a starting ratio of 100:20:1, the major band of protein was seen in particles with a hydrodynamic diameter of approximately 10 nm (Figure 1A). LCAT-treated r-HDL had a band with similar electrophoretic mobility; however, this band was more diffuse, indicating increased particle heterogeneity. The greatest size difference was found in the comparison of the 100:20:1 r-HDL with the 28:5.6:1 r-HDL. The 28:5.6:1 r-HDL were more heterogeneous and smaller, having four bands (10.7, 10, 7.5, and 7.2 nm). Upon LCAT treatment, three major bands were seen with sizes of approximately 10.5, 7.5, and 7.2 nm. The lowest of these bands (7.2 nm) may be either contaminating albumin in our apo AI preparation or lipid-free apo AI dimer, both of which migrate to this part of the gel. r-HDL made with acyl compositions other than POPC had slight but measurable differences in hydrodynamic diameter ranging from approximately 9.5 to 11 nm (Figure 1B).

Another method used to characterize our r-HDL was transmission EM (Figure 2). Both 100:20:1 starting ratio LCAT-treated and untreated r-HDL were studied. The formation of rouleaux of disks in transmission EM of nascent r-HDL was seen in all cases, confirming the discoidal shape of the starting material (Forte *et al.*, 1971). In contrast, rouleaux were not seen in preparations of r-HDL treated with

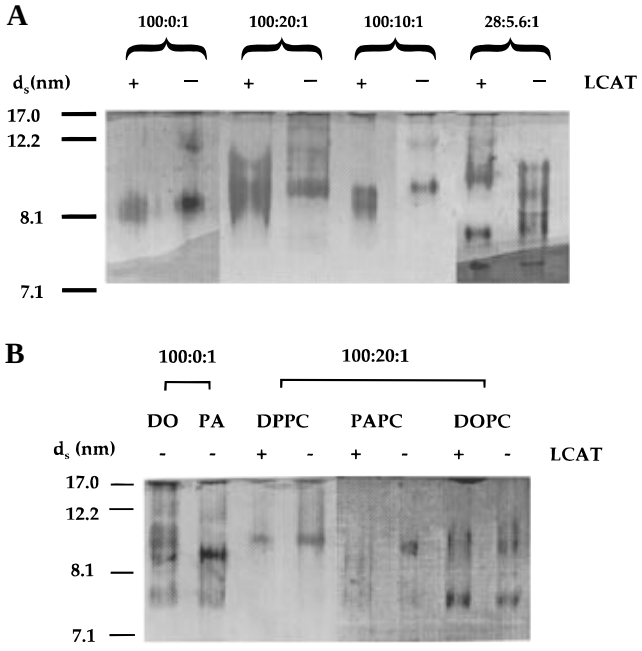

FIGURE 1: Gradient gel electrophoresis of r-HDL. Scanned images of nondenaturing 8−25% gradient gels stained with silver are shown. Gels were run for 268 AVh and stained with the Pharmacia Phast silver stain kit. Gels were scanned with a Hewlet Packard Scan Jet 4P equipped with a transparency adapter. Images were produced using Desk Scan 2 software by Hewlet Packard, Photoshop (version 4.0) by Adobe, and Powerpoint (version 4.0) by Microsoft. Panel A shows GGE run on POPC r-HDL made with different starting ratios. Panel B shows GGE of particles made with different starting ratios. In panel B, DO and PA refer to r-HDL made with either DOPC or PAPC. Standards are globular proteins of known Stokes diameter (thyroglobulin, 17.0 nm; ferritin, 12.2 nm; lactate dehydrogenase, 8.1 nm; and bovine serum albumin, 7.1 nm). See Materials and Methods for further details.

LCAT (aside from an occasional stack of two to three particles), and the particles were mainly spheroidal. Circular objects seen in micrographs of r-HDL which were not treated with LCAT are most likely discoidal particles seen on end; it is highly unlikely that spherical 100:20:1 particles would form in our discoidal particle preparations. The micrographs also showed more size distribution in the LCAT treated preparations than disks. These data are consistent with both gradient centrifugation and GGE, which reveal a wider distribution of r-HDL in the LCAT treated preparation compared to disks.

Finally, DLS was used to characterize these r-HDL (Table 4). A typical size distribution had a mean diameter of 11 nm. Analysis of the particle distribution showed a peak width of 5 nm at half-peak height, an indication of our particle heterogeneity as seen with other techniques. DLS studies indicate that LCAT treated and untreated r-HDL in solution had size distributions comparable to those seen on nondenaturing GGE.

The properties of the r-HDL preparations are summarized in Table 4. The third and fifth columns of Table 4 (GGE and DLS) relate the hydrodynamic diameter of the corresponding spheroidal r-HDL. Column four, based on EM, gives the separate length and width dimensions, not the average diameter, of the r-HDL, providing in this instance more shape information than the other techniques. It is known by the work of Gantz *et al.* (1991) that spherical lipoprotein particles flatten out somewhat during EM staining and preparation. This may explain the size discrepancy

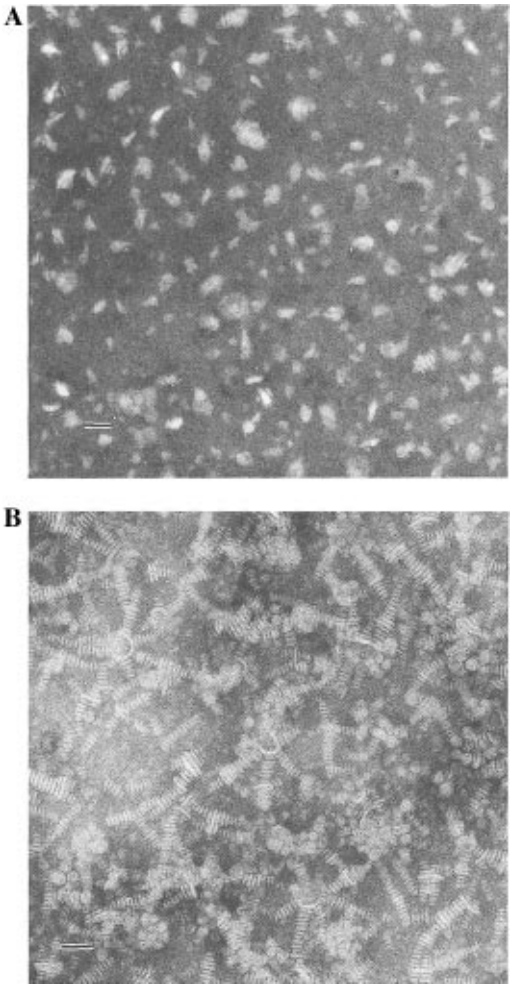

FIGURE 2: Transmission EM. Transmission electron micrographs were taken of LCAT-treated (panel A) and untreated (panel B) 100:20:1 POPC r-HDL. Representative micrographs are shown. Untreated r-HDL show rouleaux formation, indicating disk-shaped particles. LCAT-treated r-HDL reveal more spheroidal and heterogeneous particles. The bar in each micrograph indicates 35 nm. Conditions were described under Materials and Methods.

between EM and our other techniques. The sixth column presents the hydrodynamic diameters calculated for each type of r-HDL by summing the total molecular volume of all components in the particle (Jonas *et al.*, 1990) and assuming the diameter based on the volume of a disk with thickness of 4.5 nm for the untreated r-HDL or the volume of a sphere for the LCAT treated r-HDL. Each particle was assumed to have two molecules of apo AI (Sparks *et al.*, 1992). Calculated values were in close agreement with those observed in our experimental methods.

Collectively, these data show that our r-HDL particles are more homogeneous than native HDL and are in the proper size range (10−11 nm). All characterization techniques employed were in close agreement with each other. Upon treatment with LCAT, discoidal particles change in conformation to spheroidal particles rich in CE. These discoidal and spheriodal particles faithfully model nascent and mature HDL particles, respectively.

Hydrolysis. The r-HDL characterized in Tables 1−3 were used as substrates for HL. A time course of PC hydrolysis was performed using POPC r-HDL made with the 100:20:1 starting ratio (Figure 3). At the initial time point, 15 min, the rates of hydrolysis were comparable for LCAT-treated

Table 4: Size of POPC Particles As Determined by Four Different Techniques

starting ratio, PC:FC:AI	LCAT	GGE	EM	DLS	calculated
100:0:1	+	10			9.0
	−	10			10.7
100:10:1	+	10			9.5
	−	10			11.5
100:20:1	+	10	(25.2 ± 17.9) × (10.1 ± 3.9)	11.1 ± 1	9.8
	−	10	(16.5 ± 5.6) × (5.2 ± 0.4)	11.4 ± 1.1	11.6
28:5.6:1	+	7.5			8.0
	−	7.5			8.7

[a] The r-HDL listed in Table 1 were sized using up to four different techniques. LCAT indicates whether the r-HDL were treated with LCAT (+) or left untreated (−). All sizes listed are in nanometers for the hydrodynamic diameter of the r-HDL except for EM which gives both the long and short axis of each particle seen. Techniques used are described in detail under Methods. Values given are expressed as mean ± SEM.

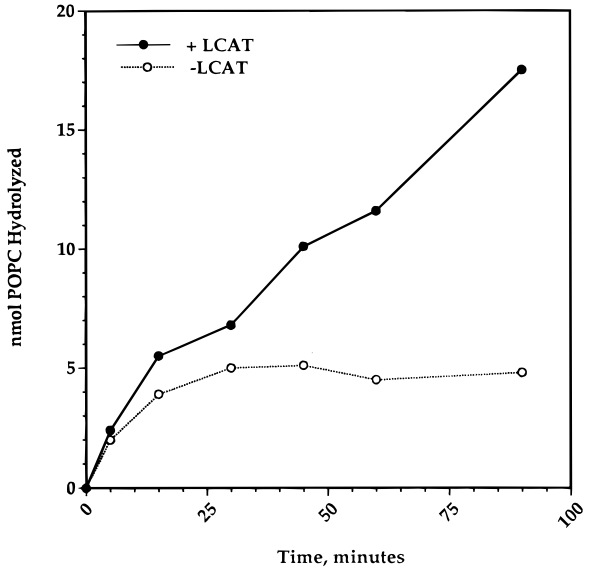

FIGURE 3: Time course of PC hydrolysis by HL. 200 nmol of r-HDL POPC was hydrolyzed by 0.6 μg of HL using the conditions described under Materials and Methods for incubation times ranging from 5 to 90 min. LCAT-treated (filled circles) and untreated particles (open circles) were hydrolyzed. Values expressed as nanomoles of PC hydrolyzed. A representative experiment (an average of duplicates) is shown. The specific activity of HL used in this figure was 43 μmol min^{-1} mg^{-1}. In all other figures, the specific activity was 133 μmol min^{-1} mg^{-1}.

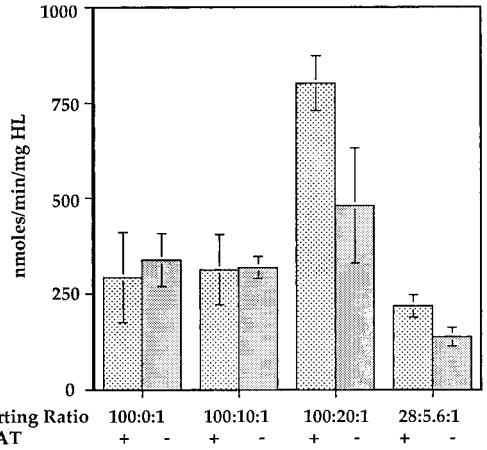

FIGURE 4: Effect of composition and size on r-HDL PC hydrolysis. 200 nmol of POPC containing r-HDL with the compositions shown in Table 1 was hydrolyzed using 0.6 μg of HL and incubation times of 60 min as described under Materials and Methods. Two (100:10:1 and 28:5.6:1 ratios) or four (100:0:1 and 100:20:1) experiments were performed in duplicate. Values shown are mean ± standard error of the mean.

and untreated r-HDL. After 30 min, there was little further hydrolysis seen with the untreated r-HDL while the hydrolysis of LCAT-treated particles remained linear throughout the length of the time course (90 min). It is possible that the hydrolysis seen up to 15 min with the r-HDL minus LCAT is due to the presence of a small percentage (2−3%) of nondiscoidal particles. This could account for the nonlinear kinetics but would imply that discoidal substrate is not hydrolyzed to an appreciable extent, if at all. A second explanation is that each discoidal r-HDL has 2−3% of its PC available for hydrolysis and above this percentage hydrolysis does not occur.

An attempt was made to saturate HL with substrate. The amount of substrate ranged up to 300 nmol of PC. Hydrolysis was linear with respect to increasing substrate concentration through both ranges assayed (data not shown). We were, however, unable to saturate HL using either preparation of r-HDL since we were limited by the amount of substrate available. Based on the above results, we used 200 nmol of r-HDL PC as our standard hydrolysis conditions in the remaining experiments.

The effect of size and composition on r-HDL PC hydrolysis by HL was next determined (Figure 4). Two major effects were noted. The most obvious result was the finding that the spheroidal, CE-rich r-HDL were degraded at a faster rate by HL than untreated 100:20:1 r-HDL. The second significant finding was found comparing particles made with the 100:20:1 and 28:5.6:1 ratios (same starting PC to UC ratio). When compared with smaller lipid poor r-HDL, the larger lipid-rich r-HDL were hydrolyzed up to 4-fold more rapidly. This was true for both LCAT-treated and untreated samples. Treatment by LCAT alone did not have an effect on the 100:0:1 or 100:10:1 r-HDL. We believe that the effect seen with LCAT in the treated 100:20:1 r-HDL was due to the higher level of CE and corresponding shape change seen in these r-HDL compared to the 100:0:1 or 100:10:1. Also, in contrast to studies performed on monomolecular films, UC had no effect on r-HDL hydrolysis (Wilcox *et al.*, 1993). In order to study the effect of CE on hydrolysis further, we treated samples of r-HDL with Triton-X-100 (final molar ratio of 1:5, r-HDL PC:Triton-X-100) (Figure 5). By treating the particles with Triton, we converted all r-HDL into mixed micelles. All effects of conformation on hydrolysis should be eliminated in these mixed micelles. The lipid and protein components of either the discoidal or the spheriodal r-HDL are diluted in a detergent matrix such that any effect of CE on hydrolysis can be studied independently of particle conformation. Using these micelles, we determined that CE

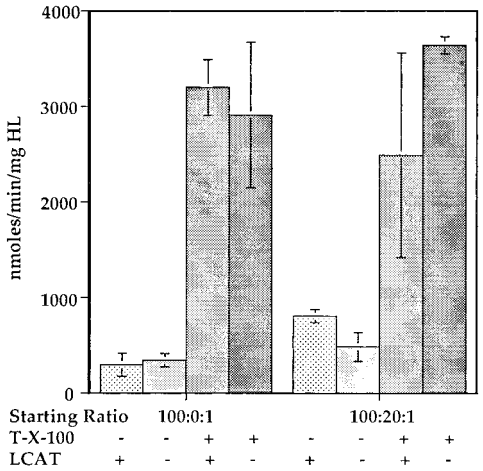

FIGURE 5: Effect of Triton X-100 on particle PC hydrolysis. 200 nmol of r-HDL POPC was treated with 1 μmol of Triton X-100 (samples were vortexed for 1 min) and hydrolyzed using 0.6 μg of HL and incubation times of 60 min as described under Materials and Methods. Two experiments were performed in duplicate. Values shown are mean ± standard error of the mean.

by itself had no effect on HL; when Triton was added, hydrolysis increased up to 10 fold in all r-HDL preparations assayed, further supporting the hypothesis that the packing of PC in the particle plays a major role in hydrolysis.

DLS was performed on LCAT-treated and untreated 100:20:1 particles to see if a change in hydrodynamic diameter occurred during HL hydrolysis. Hydrolysis conditions were the same as was noted under Methods except the temperature was decreased to 25 °C and the incubation time was increased to 2 h. Extents of hydrolysis were comparable to other 100:20:1 particles. No significant change in the hydrodynamic diameter of these particles was observed, indicating fusion of particles to larger sizes did not occur (data not shown).

The effect of PC acyl composition on HL activity was next investigated. The experiments in Tables 2 and 3 were carried out with two preparations of HL that had different specific activity in control assays (monoglyceride used as substrate). In Table 2, a comparison is shown of the hydrolysis of DOPC, PAPC, and DPPC in r-HDL disks prepared without UC and with similar final ratios of PC to AI. We observed that 280 and 190 nmol/min^{-1} (mg of HL)$^{-1}$ of DOPC and PAPC, respectively, were hydrolyzed but this difference was only in the 56th percentile confidence interval (based on a paired *t*-test). DPPC was not hydrolyzed to a measurable extent. Next a comparison of particles formed with UC was made (Table 3). In these r-HDL, less UC and CE was found in DOPC, PAPC, and DPPC containing particles, partially due to decreased incorporation of UC and partially due to a lower LCAT activity with those species of PC. As was seen in r-HDL made without UC, no difference was noted in the hydrolysis of untreated POPC, PAPC, and DOPC disks made with UC. However, a difference was seen in the particles treated with LCAT; POPC particles were hydrolyzed at a faster rate than PAPC particles. DOPC hydrolysis, however, was not statistically different from POPC or PAPC. In all cases, the hydrolysis of DPPC was too low to quantitate.

DISCUSSION

Our work shows that HL preferentially hydrolyzed PC in spheroidal, CE-rich r-HDL when compared to PC in disks. These results support our hypothesis that the spheriodal r-HDL produced by LCAT treatment were more readily hydrolyzed as the result of the packing of the PC in the r-HDL. This conclusion was predicted by monolayer work in which HL was shown to be more active at a lower surface pressure (15−25 mN/m) than at a higher one (30 mN/m)-(Thuren *et al.*, 1992). In the disk PC molecules are thought to be arranged in a planar bilayer. Conversely, in a nondiscoidal r-HDL, the CE forms a core in the center of the bilayer and produces a curved surface. It should be noted, however, that levels of CE less than about 12% were not adequate to stimulate hydrolysis. As a consequence, one would predict a decrease in the lateral surface pressure at the ester bond facilitating HL penetration and hydrolysis (Thuren *et al.*, 1992). This predicted decrease in pressure could also result from removal of UC from the bilayer (Ibdah *et al.*, 1989). LCAT treatment by itself, in particles made without UC, had no effect on r-HDL PC hydrolysis by HL. Particles made with species of PC other than POPC did not incorporate as much UC and had less than 10% CE following treatment with LCAT. These r-HDL did not show an increase in hydrolytic rate compared to untreated r-HDL.

It is possible that changes in apo AI structure also contribute to the increase in hydrolysis in LCAT-treated r-HDL. Differing apo AI conformations and charges in disks and spheres have been studied by many groups (Sparks *et al.*, 1992; Jonas *et al.*, 1990; Rye & Barter, 1994; Davidson *et al.*, 1993). However, conditions that change apo AI structure, such as the UC content of the particle (Bergeron *et al.*, 1995; Sparks *et al.*, 1993), were not found to impact hydrolysis by HL in r-HDL. Additionally, data from Thuren *et al.* (1990, 1992) show no effect of apo AI on HL hydrolysis in monolayer and mixed micelle systems. Since the monolayer and mixed micelle systems present substrate and AI in widely differing conformations and HL is not affected, we feel AI does not play as important a role as it may in the activation of other enzymes, such as LCAT.

A difference in hydrolysis was noted in the comparison of large, protein-poor (100:20:1 starting ratio) particles to small, protein-rich particles (28:5.6:1 starting ratio). This could be due to the particle substrate pool size of the larger r-HDL. If the overall rate-limiting step in hydrolysis is the association−dissociation of the enzyme to r-HDL (binding of HL to r-HDL), rather than the catalytic step (binding and hydrolysis of individual molecules of phospholipid), then the faster rate of hydrolysis would be expected in particles with the largest substrate pool. That is to say that more hydrolytic events would occur before dissociation of the enzyme from the particle. Also, it may be that smaller r-HDL provide less "free" substrate for HL. If each molecule of apo AI binds a number of molecules of PC tightly and, as a consequence, renders them unavailable as substrate for HL, then a higher percentage of PC in the large particle would be available as substrate for HL compared to the small particle.

We found no effect of UC on PC hydrolysis in concentrations ranging from 0 to 17 mol%. On the other hand, data from our laboratory showed that at concentrations of UC up to 12% the hydrolysis of PE monolayers by HL was inhibited but at 15 mol % UC full activity was restored (Wilcox *et al.*, 1993). Direct comparisons of these model systems are complicated by the fact that the monolayer studies were performed on a PE monolayer without apo AI which could

be influenced differently by UC than a monolayer of PC. Likewise, Azema found modifying HDL by the addition of UC increased HL activity on PE by 30−60%; the activity, however, dropped below control values once the UC levels exceeded a 0.2:1 ratio of UC:PC (Azema *et al.*, 1990).

A number of studies in the literature have analyzed the acyl chain specificity of HL. In our studies, we compared species of PC with a saturated acyl chain in the 1 position (palmitate) and either saturated (palmitate), unsaturated (oleate), or polyunsaturated (arachidonate) in the 2 position. We also studied a PC made with two unsaturated acyl chains (dioleate). Our results using r-HDL extend those of Laboda *et al.* (1986). In their monolayer studies, DOPC was hydrolyzed to the same extent as POPC, but both were hydrolyzed to a much greater extent than DPPC. In the r-HDL model, we found PAPC was not hydrolyzed as well as POPC but better than DPPC. These results are also similar to the work of Miller *et al.* (1981), who showed that oleoylglycerol was hydrolyzed by HL 1.2-fold faster than linoleoylglycerol, but both were hydrolyzed almost 20-fold greater than stearoylglycerol. An indication of HL's ability to hydrolyze acyl chains of differing length comes from the work of Decklebaum *et al.* (1990). In those studies, emulsions of medium-chain triglycerides were hydrolyzed at a 2-fold higher rate than long-chain triglycerides. Kadowaki *et al.* (1993) showed that increased acyl chain length or inclusion of a saturated fatty acid in the *sn*-2 position decreased PC hydrolysis in r-HDL; however, these studies were only performed on spheroidal r-HDL that contained a variety of lipid and protein components. The lack of reactivity of HL with DPPC may be due to a number of factors. The packing of the DPPC in r-HDL disks and spheroids may prevent HL from binding to the r-HDL particle. While this is untested in the system employed here, data from other groups argue against this possibility. Although hydrolysis of DPPC monolayers occurs at a slower rate than POPC monolayers, binding of HL to the monolayer is largely unaffected (Laboda *et al.,* 1986). A more likely argument is that the individual molecules of DPPC cannot bind the active site of HL. In studies by Miller *et al.*, rates of hydrolysis of saturated monoglycerides were much lower than unsaturated monoglycerides in a Triton X-100 mixed micelle. In this case, bulk interactions of PC with HL would be minimal compared to the interactions of HL with Triton in the micelle (1981).

HDL is thought to be responsible for the delivery of cholesterol from peripheral tissues to the liver. Selective uptake of CE from HDL into human hepatocytes has been demonstrated using primary cultures of hepatocytes (Rinninger *et al.*, 1994). We postulate that spheroidal HDL rich in CE would preferentially deliver CE to the liver whereas discoidal, nascent HDL would not function well in this task. Native HDL leaves the liver sinusoids and goes into the circulation where they take up UC. This UC is then esterified by LCAT to form a CE rich spheriodal particle. Only following this enrichment in CE and change in conformation can the particle be effectively hydrolyzed by HL and have its CE internalized by the hepatocyte. We postulate that this mechanism prevents the premature metabolism of HDL by the liver. Similarly, since HL is known to hydrolyze the PL in HDL and contribute to HDL catabolism (Bamberger *et al.*, 1985; Marques-Vidal *et al.*, 1994; Homanics *et al.*, 1995; Fan *et al.*, 1994), high levels of HL may lead to low HDL levels. Since HDL cholesterol levels are inversely related with the risk of developing atherosclerosis, low levels of HDL may be atherogenic. However, based on data from other laboratories which show a positive correlation of HL level and decreased risk of atherosclerosis (Busch *et al.*, 1994,; Fan *et al.*, 1994), we postulate that, in this instance, the role of HL is anti-atherogenic in that HL increases hepatic uptake of CE from plasma. This hypothesis is supported by the work of Dugi *et al.*, who have shown an inverse correlation of HL with atherosclerosis in familial hypercholesterolemic patients.

We have demonstrated that r-HDL particles model native HDL in both size and composition but are less heterogeneous than native HDL. We feel they will be a useful model system for studying the interactions of HDL with HL in the future.

REFERENCES

Albers, J. J., Chen, C., & Lacko, A. G. (1986) *Methods Enzymol. 129*, 763−783.

Azema, C., Marques-Vidal, P., Lespine, A., Simard, G., Chap, H., & Perret, B. (1990) *Biochim. Biophys. Acta 1046*, 73−80.

Babiak, J., Tamachi, H., Johnson, F. L., Parks, J. S., & Rudel, L. L. (1986) *J. Lipid Res. 27*, 1304−1317.

Bamberger, M., Glick, J. M., & Rothblat, G. H. (1983) *J. Lipid Res. 24*, 869−876.

Bamberger, M., Lund-Katz, S., Phillips, M. C., & Rothblat, G. H. (1985) *Biochemistry 24*, 3693−3701.

Bergeron, J., Frank, P. K., Scales, D., Meng, Q., Castro, G., & Marcel, Y. L. (1995) *J. Biol. Chem. 270*, 27429−27438.

Breckenridge, W. C., Little, J. A., Alaupovic, P., Wang, C. S., Kuksis, A., Lindgren, F., & Gardiner, G. (1982) *Atherosclerosis 45*, 161−179.

Brewer, H. B., Ronan, R., Meng, M., & Bishop, C. (1986) *Methods Enzymol. 128*, 223−247.

Busch, S. J., Barnhardt, R. L., Martin, G. A., Fitzgerald, M. C., Yates, M. T., Mao, S. J. T., Thomas, C. E., & Jackson, R. L. (1994) *J. Biol. Chem. 269*, 16376−16382.

Connelly, P. W., Maguire, G. F., Lee, M., & Alick Little, J. (1990) *Arteriosclerosis 10*, 40−48.

Davidson, W. S., Sparks, D. L., Lund-Katz, S., & Phillips, M. C. (1994) *J. Biol. Chem. 269*, 8959−8965.

Deckelbaum, R. J., Hamilton, J. A., Moser, A., Bengtsson-Olivecrona, G., Butbul, E., Carpentier, Y. A., Gutman, A., & Olivecrona, T. (1990) *Biochemistry 29*, 1136−1142.

Dugi, K. A., Feuerstein, I. M., Hill, S., Shih, J., Santamarina-Fojo, S., Brewer, H. B., & Hoeg, J. M. (1997) *Atheroscler., Thromb. Vasc. Biol. 17*, 354−364.

Ehnholm, C., & Kuusi, T. (1986) *Methods Enzymol. 129*, 716−738.

Eisenberg, S. (1984) *J. Lipid Res. 25*, 1017−1058.

Fan, J., Wang, J., Bensadoun, A., Lauer, S. J., Dang, Q., Mahley, R. W., & Taylor, J. M. (1994) *Proc. Natl. Acad. Sci. U.S.A. 91*, 8724−8728.

Forte, T., Norum, K. R., Glomset, J. A., & Nichols, A. V. (1971) *J. Clin. Invest. 50*, 1141−1148.

Gantz, D., Bennet Clark, S., Derksen, A., & Small, D. A. (1991) *J. Lipid Res. 31*, 163−171.

Goldberg, I. J., Mazlen, G. R., Rubinstein, A., Gibson, J. C., Paterniti, J. R., Lindgren, F. T., & Brown, W. V. (1985) *Metabolism 34*, 832−835.

Gordon, D. J. (1990) *Endocrinol. Metab. Clin. North Am. 19*, 299−309.

Hamilton, R. L., Williams, M. C., Fielding, C. J., & Havel, R. J. (1976) *J. Clin. Invest. 58*, 667−680.

Hantgan, R. R., Bratten, J. V., & Rocco, M. (1993) *Biochemistry 32*, 3935−3941.

Hegele, R. A., Alick Little, J., Vezina, C., Maguire, G. F., Tu, L., Wolever, T. S., Jenkins, D. J. A., & Connelly, P. W. (1993) *Arterioscler. Thromb. 13*, 720−728.

Homanics, G. E., de Silva, H. V., Osada, J., Zhang, S. H., Wong, H., Borensztajn, J., & Maeda, N. (1995) *J. Biol. Chem. 270*, 2974−2980.
Ibdah, J. A., Lund-Katz, S., & Phillips, M. C. (1989) *Biochemistry 28*, 1126−1133.
Johnson, F. L., Babiak, J., & Rudel, L. L. (1986) *J. Lipid Res. 27*, 537−548.
Jonas, A., Hefelde Wald, J., Harms Toohill, K. L., Krul, E. S., & Kezdy, K. E. (1990) *J. Biol. Chem. 265*, 22123−22129.
Jensen, G. L., & Bensadoun, A. (1981) *Anal. Biochem. 113*, 246 (1981).
Kadowaki, H., Patton, G. M., & Robins, S. J. (1992) *J. Lipid Res. 33*, 1689−1698.
Kadowaki, H., Patton G. M., Robins, S. J. (1993) *J. Lipid Res. 34*, 180−189.
Kuusi, T., Nikkila, E. A., Virtanen, I., & Kinnunen, P. K. J. (1979) *Biochem. J. 181*, 245−246.
Laboda, H. M., Glick, J. M., & Phillips, M. C. (1986) *Biochim. Biophys. Acta 876*, 233−242.
Lowry, O. H., Rosebrough, N. J., Farr, A. L., & Randall, R. J. (1951) *J. Biol. Chem. 193*, 265−275.
Marques-Vidal, P., Azema, C., Collet, X., Veiu, C., Chap, H., & Perret, B. (1994) *J. Lipid Res. 35*, 373.
McCall, M. R., Nichols, A. V., Morton, R. E., Blanche, P. J., Shore, V. G., Hara, S., & Forte, T. M. (1993) *J. Lipid Res. 34*, 37−48.
Miller, G. J., & Miller N. E. (1975) *Lancet 1*, 16−19.
Miller, C. H., Parce, J. W., Sisson, P., & Waite, M. (1981) *Biochim. Biophys. Acta 665*, 385−392.
Nichols, A. V., Blanche, P. J., Gong, E. L., Shore, V. G., & Forte, T. M. (1985) *Biochim. Biophys. Acta 834*, 285−300.
Patel, K. M., Morriset, J. D., & Sparrow, J. T. (1979) *Lipids 14*, 596−597.
Peterson, G. L. (1977) *Anal. Biochem. 83*, 346−356.
Provencher, S. W. (1982) *Comput. Phys. Commun. 27*, 229.
Rinninger, F., Brundert, M., Jackle, S., Galle, P. R., Busch, C., Izbicki, J. R., Rogiers, X., Henner-Bruns, D., Kremer, B., Broelsch, C. E., & Greten, H. (1994) *Hepatology 19*, 1100−1114.
Rye, K.-A., & Barter, P. J. (1994) *J. Biol. Chem. 269*, 10298−10303.
Scobey, M. W., Johnson, F. L., & Rudel, L. L. (1989) *Am. J. Physiol. 257*, G644−G652.
Sparks, D. L., Phillips, M. P., & Lund-Katz, S. (1992) *J. Biol. Chem. 267*, 25830−25838.
Sparks, D. L., Davidson, W. S., Lund-Katz, S., & Phillips, M. P (1993) *J. Biol. Chem. 268*, 23250−23257.
Thuren, T., Wilcox, R. W., Sisson, P., & Waite, M. (1990) *J. Biol. Chem. 266*, 4853−4861.
Thuren, T., Weisgrabber, K. H., Sisson, P., & Waite, M. (1992) *Biochemistry 31*, 2332−2338.
Vanio, P., Virtanen, J. A., Kinnunen, P. K. J., Voyta, J. C., Smith, L. C., Gotto, A. M., Sparrow, J. T., Pattus, F., & Verger, R. (1983) *Biochemistry 22*, 2270−2275.
Verdery, R. B., & Nichols A. V. (1975) *Chem. Phys. Lipids 14*, 123−134.
Waite, M., & Sisson, P. (1973) *J. Biol. Chem. 243*, 7201−7206.
Waite, M., Thuren, T. Y., Wilcox, R. W., Sisson, P. J., & Kuchera, G. L. (1991) *Methods Enzymol. 197*, 331−339.
Wilcox, R. W., Thuren, T., Sisson, P., Schmitt, J. D., Kennedy, M., & Waite, M. (1993) *Biochemistry 32*, 5752−5758.

BI970356W